

## THE SPIN DENSITY DISTRIBUTION AND THE G-TENSOR FOR THE IONS OF PYRACENE

BY

D. J. M. FASSAERT and E. DE BOER

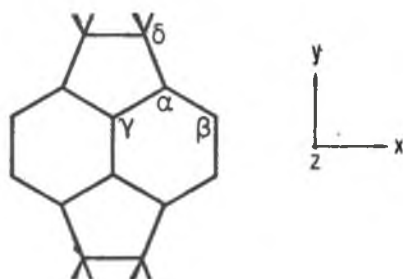
(Department of Physical Chemistry, University of Nijmegen, Nijmegen, The Netherlands)

All  $^{13}\text{C}$  hyperfine splitting constants (h.f.s.c.'s) in the negative ion of pyracene have been determined. In order to obtain the  $^{13}\text{C}$  h.f.s.c. of the carbon atom in the  $\text{CH}_2$  groups it was necessary to measure on pyracene enriched in this position with  $^{13}\text{C}$ . From these  $^{13}\text{C}$  h.f.s.c.'s together with the already known proton splitting constants, an experimental map of the spin distribution in the anion could be obtained. The influence of the two ethylene bridges on the spin distribution is discussed in terms of hyperconjugation and induction. The conclusion has been reached that both effects play an important role and that a combined model gives a reasonable description of the changes in the spin distribution, caused by the  $\text{CH}_2$  groups.

From line-broadening effects the sign of the h.f.s.c. of the  $^{13}\text{C}$  nucleus in the  $\text{CH}_2$  groups has been determined in both the anion and in the cation. Analysis of the line widths using the theory of *Freed* and *Fraenkel* resulted in the determination of the sign of the difference between the in-plane g-tensor components. This difference changed sign on going from the negative to the positive ion, in agreement with *Stone's* theory.

### Introduction

The negative and positive ions of pyracene (see structure diagram) have been studied in great detail with ESR spectroscopy<sup>1</sup>.



Structure diagram of pyracene.

<sup>1</sup> J. L. Sommerdijk and E. de Boer, 'Ion pairs in organic reactions', John Wiley and Sons, Inc., editor M. Szwarc, 1971.

In many aspects the proton ESR spectra revealed interesting features, viz. line width alternation in the spectrum of the negative ion<sup>2</sup> and second order hyperfine splitting in the spectrum of the positive ion<sup>3</sup>.

The large splitting, exhibited by the aliphatic protons, which in the positive ion is even twice as large as in the negative ion, has aroused interest from theorists. It is now generally accepted that this large splitting is brought about by hyperconjugation<sup>4</sup>. Since the carbon skeleton of pyracene is planar<sup>5</sup> it is an ideal case for the study of this effect<sup>6</sup>. The hyperfine splitting constant (h.f.s.c.) of the aromatic  $\beta$ -protons in the negative ion is substantially less than in the negative ion of naphthalene. It was suggested that this was caused by the inductive behaviour of the two ethylene bridges.

In order to study the effects of hyperconjugation and induction on the spin distribution in the ions of pyracene in detail, more experimental information should be available on the spin density distribution. This could be obtained by measuring the  $^{13}\text{C}$  h.f.s.c.'s, which are known to be a sensitive function of the spin distribution.

To achieve this, spectra were measured under high amplification and modulation and under maximum admissible concentration. In this way two  $^{13}\text{C}$  h.f.s.c.'s were measured for the anion. The h.f.s.c. of  $^{13}\text{C}$  in the  $\delta$ -position was obtained from an enriched sample. From the spectra not only the values of the h.f.s.c.'s for the  $^{13}\text{C}$  atom in the  $\delta$ -position emerged, but also the sign of the splitting constants. The  $^{13}\text{C}$  h.f.s.c.'s together with the observed proton splittings enabled us to map the complete spin density distribution in the anion of pyracene.

This could not be achieved for the positive ion, due to an insufficient signal to noise ratio in the ESR spectra. Only the magnitude and sign of the  $^{13}\text{C}$  h.f.s.c. of the  $^{13}\text{C}$  nucleus in the  $\delta$ -position were found.

For the negative ion the influence of hyperconjugation and induction on the spin density distribution is discussed by comparing the experimental spin density distribution with that of the naphthalene anion and by carrying out spin density calculations according to the hyperconjugative and the inductive models and a combination of these two.

The ESR spectra of both the anion and cation show broadening effects, caused by the anisotropic dipolar electron-nuclear interaction and by the g-tensor interaction. From this the sign of the difference between the in-

<sup>2a</sup> E. de Boer and E. L. Mackor, *J. Am. Chem. Soc.* **86**, 1513 (1964);

<sup>b</sup> E. de Boer, *Rec. Trav. Chim.* **84**, 609 (1965).

<sup>3</sup> E. de Boer and E. L. Mackor, *Mol. Phys.* **5**, 493 (1962).

<sup>4a</sup> J. R. Bolton, A. Carrington and A. D. McLachlan, *Mol. Phys.* **5**, 31 (1962);

<sup>b</sup> M. J. S. Dewar, 'Hyperconjugation', Ronald Press Co., New York, 1962.

<sup>5</sup> G. L. Simmons and E. C. Lingafelter, *Acta Cryst.* **14**, 872 (1961).

<sup>6</sup> J. P. Colpa and E. de Boer, *Mol. Phys.* **7**, 333 (1964).

plane  $g$ -tensor components could be determined. It appeared that  $(g_x - g_y)$  (see structure diagram) is negative for the anion and positive for the cation, in agreement with the predictions of Stone<sup>7</sup>.

### Experimental part

The negative ions of pyracene and pyracene-<sup>13</sup>C\*, containing 52% <sup>13</sup>C in the  $\delta$ -position were prepared by standard procedures<sup>8</sup>. As solvent 1,2-dimethoxyethane (DME) was used, with sodium as reducing agent. The positive ion of pyracene was obtained by reaction with 96% sulphuric acid, and in a mixture of SO<sub>2</sub> and BF<sub>3</sub><sup>9</sup>.

The ESR spectra were measured with a Varian V 4502 X-band spectrometer, equipped with a variable temperature control and a fieldial. The magnetic field was measured with an AEG gaussmeter and the frequency was monitored with a Hewlett Packard 5245 L frequency counter. The spectra were recorded under slow scanning conditions (about 500 mOe/min.). The signs of the hyperfine splitting constants (h.f.s.c.'s) were inferred from hyperfine lines characterized by only one magnetic quantum number unequal to zero and well separated from other hyperfine lines, so that overlap corrections could be avoided. These hyperfine lines are denoted as 'principal hyperfine lines'.

### Results

#### 1. Pyracene

Fig. 1 shows the central part of the ESR spectrum of the negative ion of pyracene-<sup>13</sup>C at -88 °C. The peaks indicated by arrows are the principal

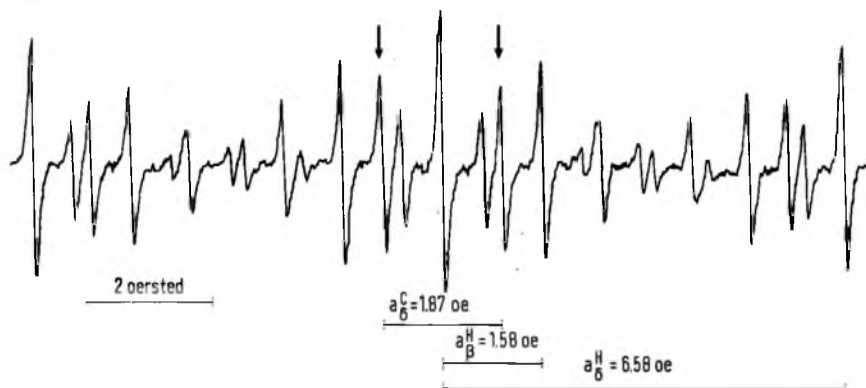


Fig. 1. The central part of the ESR spectrum of the anion of pyracene, containing 52% <sup>13</sup>C in the  $\delta$ -position (see structure diagram), measured in DME at -88 °C with Na<sup>+</sup> as counter ion. The peaks marked by arrows are <sup>13</sup>C hyperfine lines, arising from the central hyperfine line.

\*The authors wish to thank Mr. *M. J. van den Brink* of the Koninklijke/Shell Laboratorium, Amsterdam for the synthesis of normal and enriched pyracene.

<sup>7</sup> *A. J. Stone*, *ibid.* p. 311 (1964).

<sup>8</sup> *D. E. Paul*, *D. Lipkin* and *S. I. Weissman*, *J. Am. Chem. Soc.* **78**, 116 (1956).

<sup>9</sup> *H. van Willigen*, *E. de Boer*, *J. T. Cooper* and *W. F. Forbes*, *J. Chem. Phys.* **49**, 1190 (1968).

$^{13}\text{C}$  hyperfine components arising from the central hyperfine line. From the spectrum it follows that the h.f.s.c.  $|a^{\text{C}}_3| = 1.87$  Oe and that the  $^{13}\text{C}$  hyperfine line at low field has a larger peak amplitude than the high-field one. As regards the peak amplitudes of the principal  $\beta$ -proton hyperfine lines the spectrum shows that the low-field hyperfine line has a slightly higher peak height than the corresponding high-field component.

In Fig. 2 the beginning of the ESR spectrum of normal pyracene $^-$  is shown. The peak indicated by  $H_1$  is the first proton hyperfine line. The peaks denoted by greek indices are  $^{13}\text{C}$  satellites, due to  $^{13}\text{C}$  present in pyracene in its natural abundance. The peaks  $\alpha_1$ ,  $\alpha_2$  and  $\alpha_3$  are equidistant and correspond to the  $^{13}\text{C}$  satellites of the first three proton hyperfine lines

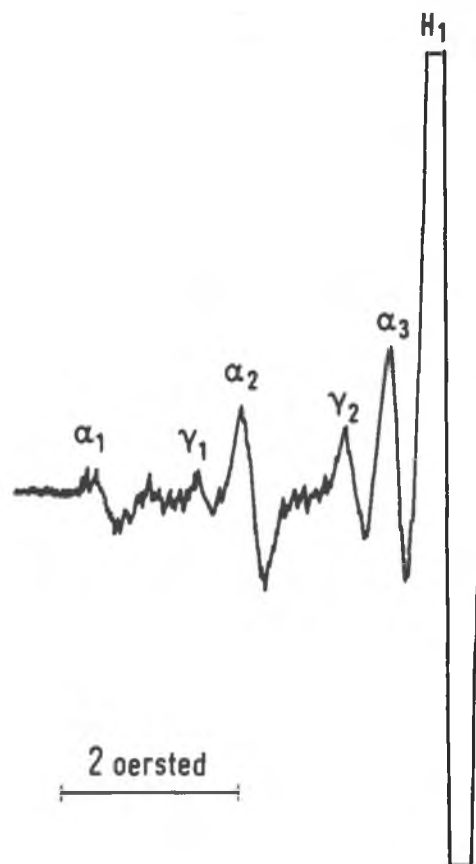


Fig. 2. The first part of the ESR spectrum of the anion of normal pyracene. For experimental conditions see Fig. 1. The peaks marked by  $\alpha$  and  $\gamma$  are  $^{13}\text{C}$  satellites of the proton peaks ( $H_1$  etc.).

arising from the four  $\beta$ -protons, separated from each other by 1.58 Oe and having an intensity ratio of 1 : 4 : 6. For the  $^{13}\text{C}$  h.f.s.c. we found 7.32 Oe. The two  $\gamma$ -peaks are also separated by 1.58 Oe and their intensities are about half the intensities of the corresponding  $\alpha_1$ - and  $\alpha_2$ -peaks. From this it can be deduced that they arise from a  $^{13}\text{C}$  nucleus in the  $\gamma$ -position (see structure diagram). The h.f.s.c.  $a_y^{\text{C}}$  amounts to 5.18 Oe. In Table I the results are tabulated, together with the h.f.s.c.'s of the negative ion of naphthalene. The assignment of the h.f.s.c. of 7.32 Oe to the  $\alpha$ -position in pyracene has been made on the basis of its close correspondence to the value of  $a_x^{\text{C}}$  in naphthalene $^-$ . The value of  $a_\beta^{\text{C}}$  has been obtained by a computer simulation of the ESR spectrum of pyracene $^-$ , taking into account all  $^1\text{H}$  and  $^{13}\text{C}$  h.f.s.c.'s and weighting the  $^{13}\text{C}$ -spectra with the percentages of natural abundance. With a value of 1.18 Oe for  $a_\beta^{\text{C}}$  the spectrum shown in Fig. 1 of ref. 2a could be matched perfectly.

Table I

$^1\text{H}$ and $^{13}\text{C}$ hyperfine splitting constants in Oersted.			
	pyracene $^-$ <sup>a</sup>	naphthalene $^-$ <sup>a</sup>	pyracene $^+$ <sup>b</sup>
$a_\alpha^{\text{H}}$		- 4.92	
$a_\beta^{\text{H}}$	(-) 1.58	- 1.82	(-) 2.00
$a_\delta^{\text{H}}$	(+) 6.58		(+) 12.8
$a_\alpha^{\text{C}}$	(+) 7.32	+ 7.26	
$a_\beta^{\text{C}}$	(-) 1.18	- 1.09	
$a_\gamma^{\text{C}}$	(-) 5.18	(-) 5.73	
$a_\delta^{\text{C}}$	- 1.87		- 2.66

The signs placed between brackets are predicted by theory, the others are determined experimentally, see ref. 16e and 22.

<sup>a</sup> Obtained in DME with  $\text{Na}^+$  at  $-70^\circ\text{C}$ .

<sup>b</sup> See ref. 3.

## 2. Pyracene $^+$ .

Fig. 3 shows the central part of the ESR spectrum of the positive ion of enriched pyracene- $^{13}\text{C}$ , dissolved in a mixture of  $\text{SO}_2$  and  $\text{BF}_3$  at  $-82^\circ\text{C}$  (upper part of the figure) and in 96% sulphuric acid at  $-10^\circ\text{C}$  (lower part of the figure).

The fine structure in the spectra is brought about by second-order hyper-

fine splitting, due to the large h.f.s.c. of the  $\alpha$ -protons,  $|a_{\alpha}^H| = 12.8$  Oe. The principal  $^{13}\text{C}$  hyperfine lines are marked by arrows. Analysis of the spectra afforded  $|a_{\gamma}^C| = 2.66$  Oe. The spectrum in  $\text{H}_2\text{SO}_4$  exhibits line-broadening effects: the  $^{13}\text{C}$  peak at low field is lower in amplitude than the peak at high field, contrary to the principal  $\beta$ -proton hyperfine lines, where the reverse is true. Efforts to observe hyperfine lines from  $^{13}\text{C}$  present in natural abundance in the  $\alpha$ -,  $\beta$ - and  $\gamma$ -positions failed.

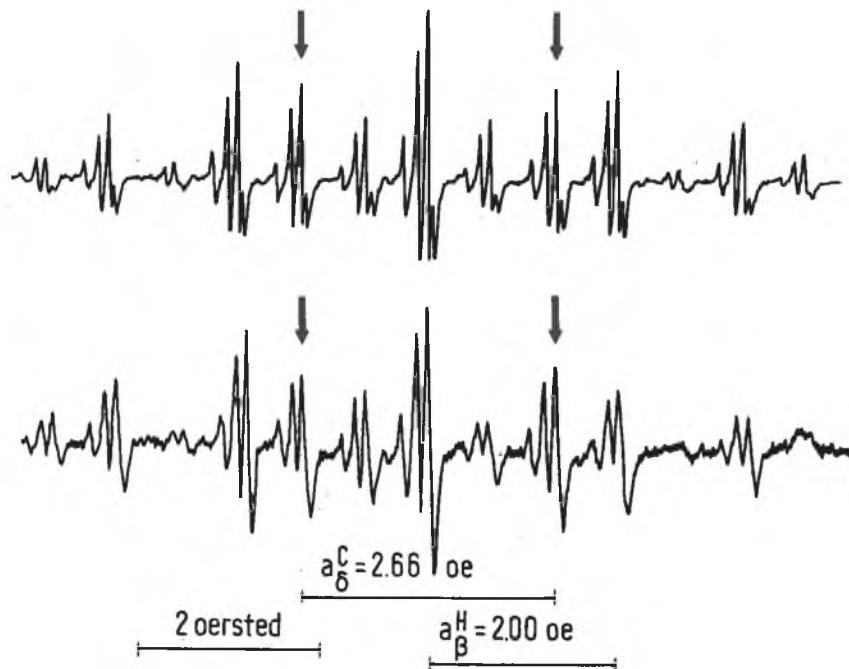


Fig. 3. The central part of the ESR spectrum of the cation of enriched pyracene- $^{13}\text{C}$ .  
 Upper part: dissolved in  $\text{SO}_2$  and  $\text{BF}_3$  at  $-82^\circ\text{C}$ .  
 Lower part: dissolved in 96% sulfuric acid at  $-10^\circ\text{C}$ .  
 The peaks marked by arrows are  $^{13}\text{C}$  hyperfine lines, arising from the central hyperfine line.

## Discussion

### 1. Spin density distribution.

The measured h.f.s.c.'s in pyracene $^-$  enable us to calculate the complete spin density distribution in this anion. As a basis for our calculations the h.f.s.c.'s  $a_{\delta}^H$ ,  $a_{\beta}^H$ ,  $a_{\alpha}^C$ ,  $a_{\gamma}^C$  and the normalization condition  $\sum \rho_i^2 = 1$  were chosen, where  $\rho_i^2$  is the spin density at carbon atom  $i$ . In our calculations we used the signs of the h.f.s.c.'s as reported in Table II. They have been

assigned according to the signs of the h.f.s.c.'s of naphthalene<sup>-</sup> (see Table I) or have been determined experimentally (*vide infra*). The spin density at carbon atom  $\beta$  has been obtained by using the *Colpa-Bolton* relation<sup>10</sup>:

$$a_{\beta}^{\text{H}} = (Q_{\text{CH}}^{\text{H}} + K_{\text{CH}}^{\text{H}} \varepsilon_{\beta}^{\pi}) \rho_{\beta}^{\pi} \quad [1]$$

where the constants  $Q$  and  $K$  are  $-27.0$  and  $-12.9$  Oe, respectively<sup>11</sup> and  $\varepsilon_{\beta}^{\pi}$  is the excess charge density on atom  $C_{\beta}$ , for which the absolute value approximately may be set equal to  $\rho_{\beta}^{\pi}$ .

The spin density on the other carbon atoms can be found from the formula of *Karplus and Fraenkel*<sup>12</sup> which, using standard notation, reads:

$$a^{\text{C}} = \left( S^{\text{C}} + \sum_{i=1}^3 Q_{\text{C}x_i}^{\text{C}} \right) \rho_{\text{C}}^{\pi} + \sum_{i=1}^3 Q_{x_i\text{C}}^{\text{C}} \rho_i^{\pi} \quad [2]$$

Values for the various parameters  $Q$  can be found in refs. 12 and 13. Finally the spin density at the aliphatic protons can be calculated from:

$$\rho_{\text{H}_2}^{\pi} = \frac{2a_{\beta}^{\text{H}}}{507} \quad [3]$$

where the value 507 refers to the h.f.s.c. of a hydrogen atom. The results are collected in Table II, together with the experimental spin densities of naphthalene<sup>-</sup>, calculated in the same way. As an internal check we used these spin densities to calculate  $a_{\beta}^{\text{C}}$ ; this afforded  $a_{\beta}^{\text{C}} = -1.09$  Oe, in good agreement with the value obtained by computer simulation.

The effect of the two ethylene bridges on the spin density distribution can be seen by comparing the experimental spin densities in pyracene<sup>-</sup> with those in naphthalene<sup>-</sup>. A reduction of spin density at the  $\alpha$ - and  $\beta$ -carbon atoms of more than 10% takes place, which is transferred mainly to the hydrogen atoms of the  $\text{CH}_2$ -groups. The spin density at the carbon atom of the  $\text{CH}_2$ -groups is small.

For the effects which substituents have on the electronic structure of molecules two distinct concepts have been used in the literature: hyperconjugation and induction<sup>4,6</sup>. In the hyperconjugative model the conjugation of the  $\pi$ -orbitals is extended to the substituents, in the inductive description the carbon atoms connected to the  $\text{CH}_2$ -groups are made more electropositive in order to account for the electron-releasing effect of the  $\text{CH}_2$ -groups. To illustrate these effects we carried out spin density calculations for pyracene<sup>±</sup> according to both models. The parameters needed for

<sup>10</sup> J. P. Colpa and J. R. Bolton, *Mol. Phys.* **6**, 273 (1963).

<sup>11</sup> J. R. Bolton, *J. Phys. Chem.* **71**, 3702 (1967).

<sup>12</sup> M. Karplus and G. K. Fraenkel, *J. Chem. Phys.* **35**, 1312 (1961).

<sup>13</sup> H. L. Strauss and G. K. Fraenkel, *ibid.*, p. 1738 (1961).

the hyperconjugative calculations can be found in ref. 6, the induction parameter was taken equal to  $-0.2\beta^{14}$ . The spin densities were calculated correct in the first order of the configuration interaction non-diagonal matrix elements, using the formula given in ref. 15, equation 4. The outcome of the calculations is listed in Table II, where, also for comparison, the first order spin densities of naphthalene<sup>±</sup> are given. The reduction of the spin density at the  $\alpha$ -carbon atom is correctly predicted by the hyperconjugative model, whereas the inductive model predicts the decrease of the spin density at the  $\beta$ -carbon atom correctly.

This suggests that both effects are needed to explain the reduction in spin density at the  $\alpha$ - as well as at the  $\beta$ -carbon atom. In Table II the results obtained by the combined model, hyperconjugation plus induction, are also listed. As was expected this model yields spin densities at the  $\alpha$ - and  $\beta$ -carbon atoms, which are indeed lower than the theoretical spin densities on the corresponding carbon atoms in naphthalene<sup>-</sup>. In addition, the ratio and the magnitude of the aliphatic h.f.s.c.'s are correctly predicted for the ions of pyracene.

No detailed discussion can be given on the spin distribution in pyracene<sup>+</sup>, because we were unable to measure all <sup>13</sup>C h.f.s.c.'s. The increase of the

Table II

Spin densities.

Position	Theoretical						Experimental		
	Pyracene <sup>-</sup>			Pyracene <sup>+</sup>			Naphthalene <sup>+</sup>	Pyracene <sup>-</sup>	Naphthalene <sup>-</sup>
	Hyp. <sup>a</sup> + Ind. <sup>b</sup>	Hyp. <sup>a</sup>	Ind. <sup>b</sup>	Hyp. <sup>a</sup> + Ind. <sup>b</sup>	Hyp. <sup>a</sup>	Ind. <sup>b</sup>			
$\rho_{\alpha}^{\pi}$	0.214	0.208	0.234	0.164	0.166	0.217	0.225	0.1719	0.1871
$\rho_{\beta}^{\pi}$	0.039	0.048	0.038	0.063	0.055	0.056	0.047	0.0603	0.0697
$\rho_{\gamma}^{\pi}$	-0.034	-0.036	-0.042	-0.036	-0.033	-0.045	-0.044	-0.0232	-0.0138
$\rho_{\delta}^{\pi}$	-0.010	-0.010	—	-0.002	-0.001	—	—	-0.0034	—
$\rho_{H_2}^{\pi}$	0.024	0.023	—	0.043	0.046	—	—	0.0260	—

<sup>a</sup> For the numerical values of the parameters used see refs. 6 and 15.

<sup>b</sup> Induction parameter  $-0.2\beta^{14}$ .

<sup>14</sup> J. P. Colpa, C. MacLean and E. L. Mackor, *Tetrahedron* **19**, 65 (1963).

<sup>15</sup> E. de Boer and J. P. Colpa, *J. Phys. Chem.* **71**, 21 (1967).



$\beta$ -proton h.f.s.c. compared with that of pyracene<sup>-</sup> is reflected in the increase of the spin density at the  $\beta$ -carbon atom going from the negative to the positive ion of pyracene (see Table II).

## 2. Signs of hyperfine splitting constants and the g-tensor.

### a. Introduction.

It has been shown<sup>16</sup> that the line widths of the ESR hyperfine components provide information on the sign of the h.f.s.c.'s and the g-tensor. The combined effect of the anisotropic dipolar electron-nuclear interaction and the g-tensor interaction causes the line widths to depend on the nuclear magnetic quantum numbers. For hyperfine lines arising from an equivalent set of nuclei and characterized by one total nuclear magnetic quantum number unequal to zero, say M, the line width parameter  $T_2$  is given by:

$$T_2^{-1} = K M^2 + L M + C \quad [4]$$

where K, L and C are parameters. The linear term in M causes peaks with the same absolute value of M to have different line widths. From this difference in line width the sign of the h.f.s.c. can be inferred<sup>16e</sup>, from the numerical value of the difference the components of the g-tensor<sup>16c</sup> can be evaluated. To obtain this information we have to calculate the parameter L. From the theory of *Freed and Fraenkel*<sup>17</sup> it follows that:

$$L = \frac{16}{3} j^{(DG)}(0) B_0 \quad [5]$$

where  $B_0$  is the external magnetic field and  $j^{(DG)}(0)$  the spectral density function, due to the cross term between the time-dependent anisotropic dipole and g-tensor interaction. For a magnetic nucleus in the i-th equivalent group  $j_i^{(DG)}(0)$  is given by<sup>18, 19</sup>:

$$j_i^{(DG)}(0) = A \left\{ \tilde{D}_i^{(0)} g^{(0)} + 2 R \tilde{D}_i^{(2)} g^{(2)} \right\} \quad [6]$$

where  $A = \frac{2\pi |\beta_e| \tau_R}{10 \hbar}$ ,  $\tau_R$  = rotational correlation time,

<sup>16a</sup> H. M. McConnell, J.Chem.Phys. **25**, 709 (1956);

b D. Kivelson, *ibid.* **27**, 1087 (1957);

c *ibid.* **33**, 1094 (1960);

d J. W. H. Scheurs and D. Kivelson, *ibid.* **36**, 117 (1962);

e E. de Boer and E. L. Mackor, *ibid.* **38**, 1450 (1963).

<sup>17</sup> J. H. Freed and G. K. Fraenkel, *ibid.* **39**, 326 (1963).

<sup>18</sup> G. K. Fraenkel, J.Phys.Chem. **71**, 139 (1967).

<sup>19</sup> B. G. Segal, A. Reymond and G. K. Fraenkel, J.Chem.Phys. **51**, 1336 (1969).

$$\begin{aligned}\bar{D}_i^{(m)} &= \frac{1}{2\pi} |\gamma_e| \gamma_I \hbar D_i^{(m)} \\ g^{(0)} &= \frac{1}{\sqrt{6}} \left[ 2g_3 - (g_1 + g_2) \right] \\ g^{(2)} &= \frac{1}{2} (g_1 - g_2)\end{aligned}$$

$g_1, g_2, g_3$  are the principal components of the  $g$ -tensor, the dipolar coefficients  $D_i^{(m)}$  are related to the anisotropic dipolar interaction and are defined in ref. 18 and  $R\bar{D}_i^{(2)}$  means the real part of  $\bar{D}_i^{(2)}$  (the  $\bar{D}_i^{(m)}$  are expressed in frequency units, Hz); the other symbols have their usual meaning. For planar aromatic radicals  $g_3$ , the component of the  $g$ -tensor perpendicular to the aromatic plane, may be set equal to  $g_e^{7,20}$ , the free electron  $g$ -value 2.002319. Then the quantity  $g^{(0)}$  reduces to:

$$g^{(0)} = \sqrt{\frac{3}{2}} (g_e - g_{iso}) \quad [7]$$

where  $g_{iso}$  is the isotropic  $g$ -value. Since the dipolar coefficients  $D_i^{(m)}$  can be computed, using the formulas of *McConnell* and *Strathdee*<sup>21</sup>, the spectral density  $j^{(DG)}(0)$  can be calculated as a function of  $g^{(2)} = \frac{1}{2}(g_1 - g_2)$ , in which  $g_1$  and  $g_2$  are the in-plane components of the  $g$ -tensor.

In the following, the superscript DG on the various  $j$ 's will be dispensed with.

#### b. *Pyracene*<sup>-</sup>.

Peak height measurements were performed on the principal hyperfine lines arising from the  $\beta$ -protons and from the <sup>13</sup>C nuclei at the  $\delta$ -position. From Fig. 1 it is clear that the peak height differences are small. This will introduce relatively large errors in the experimental  $L$  values, rendering a numerical evaluation of the in-plane  $g$ -tensor components not meaningful. However, sufficient data are available to assess the sign of  $(g_1 - g_2)$  and to determine approximately its value.

From the higher peak height of the  $\beta$ -proton principal hyperfine line at low field with respect to the corresponding component at high field and the known sign of  $a_{\beta}^H$ <sup>22</sup> (see Table I), it follows that the sign of the parameter  $L$  is positive. Hence also  $j_{\beta}^H(0)$  has to be positive and its magni-

<sup>20</sup> H. M. McConnell and R. E. Robertson, *J. Phys. Chem.* **61**, 1018 (1957).

<sup>21</sup> H. M. McConnell and J. Strathdee, *Mol. Phys.* **2**, 129 (1959).

<sup>22</sup> B. M. P. Hendriks, G. W. Canters, C. Corvaja, J. W. M. de Boer and E. de Boer, *ibid.* **20**, 193 (1971).

tude should be small ( $L$  is almost zero). Utilizing the theoretical spin densities in Table II and the isotropic  $g$ -value,  $g_{\text{iso}} = 2.00275$ , the spectral densities  $j_{\beta}^{\text{H}}(0)$  and  $j_{\delta}^{\text{C}}(0)$  have been calculated for the three different models. They are:

$$\begin{array}{l} j_{\beta}^{\text{H}}(0) = 717.2 + 139.0 (g_1 - g_2) \cdot 10^4 \\ j_{\delta}^{\text{C}}(0) = 727.5 - 53.2 (g_1 - g_2) \cdot 10^4 \end{array} \left. \begin{array}{l} \text{Hyperconjugation +} \\ \text{induction} \end{array} \right\} \quad [8a]$$

$$\begin{array}{l} j_{\beta}^{\text{H}}(0) = 731.9 + 142.7 (g_1 - g_2) \cdot 10^4 \\ j_{\delta}^{\text{C}}(0) = 728.5 - 51.7 (g_1 - g_2) \cdot 10^4 \end{array} \left. \begin{array}{l} \text{Hyperconjugation} \end{array} \right\} \quad [8b]$$

$$\begin{array}{l} j_{\beta}^{\text{H}}(0) = 741.3 + 147.5 (g_1 - g_2) \cdot 10^4 \\ j_{\delta}^{\text{C}}(0) = 282.9 - 51.1 (g_1 - g_2) \cdot 10^4 \end{array} \left. \begin{array}{l} \text{Induction} \end{array} \right\} \quad [8c]$$

(the constant factor  $A$  has been omitted).

In order for  $j_{\beta}^{\text{H}}(0)$  to be small and positive,  $(g_1 - g_2) = (g_x - g_y)$  has to be  $(-4 \text{ to } -5) \times 10^{-4}$ . For the positive ion of pyracene it was found<sup>23</sup> that  $(g_1 - g_2) = +6 \times 10^{-4}$ . Hence the difference between the in-plane  $g$ -tensor components changes sign on going from the positive to the negative ion. Theoretically this has been predicted by Stone<sup>7</sup> for ions of even-alternant molecules and experimentally this has been confirmed by us<sup>24</sup> in a recent study of the alternant ions of anthracene, tetracene and perylene. Apparently the presence of the two ethylene bridges does not disturb this theorem, which arises from the pairing relation existing between the molecular orbital coefficients of the bonding molecular orbitals in the cation and the corresponding anti-bonding molecular orbitals in the anion. Since  $(g_1 - g_2)$  is negative for pyracene<sup>-</sup>,  $j_{\delta}^{\text{C}}(0)$  will be positive, irrespective of which model one uses for the calculation of the spin densities. From this, together with the observed higher peak height of the <sup>13</sup>C hyperfine component at low field with respect to the corresponding component at high field, it follows that the sign of  $a_{\delta}^{\text{C}}$  is negative.

It is interesting to note that the first term in the spectral density is strongly influenced by the spin density on the considered nucleus itself. This is clearly manifested by computing the spectral densities, using the experimental spin densities:

$$j_{\beta}^{\text{H}}(0) = 698.1 + 137.0 (g_1 - g_2) \cdot 10^4 \quad [9a]$$

$$j_{\delta}^{\text{C}}(0) = -29.4 - 40.04 (g_1 - g_2) \cdot 10^4 \quad [9b]$$

<sup>23</sup> E. de Boer and E. L. Mackor, Proceedings of the XIth Colloque Ampère, p. 339, Eindhoven, 1962.

<sup>24</sup> D. J. M. Fassaert and E. de Boer, Mol. Phys. 21, 485 (1971).

Contrary to  $j_{\beta}^{\text{H}}(0)$ ,  $j_{\delta}^{\text{C}}(0)$  changes drastically. This is caused primarily by the spin density on the  $^{13}\text{C}$  nucleus itself, which contributes to  $D_1^{(0)}$  a term equal to  $\frac{1}{5} \langle r^{-3}_{\delta} \rangle \rho_{\delta}^{\pi}$ <sup>18</sup>, where  $\langle r^{-3} \rangle$  is the expectation value of  $r^{-3}_{\delta}$  over the atomic  $2p_{\pi}$ -function on  $^{13}\text{C}$  atom  $\delta$ . Using a *Hartree-Fock* function Bolton and Fraenkel<sup>25</sup> calculated for this local contribution to  $\bar{D}_{\text{C}_{\delta}}(0)$ :

$$\bar{D}_{\text{C}_{\delta}}(0)(\text{local}) = 111.2 \times 10^6 \rho_{\delta}^{\pi} \quad [10]$$

In spite of this, the conclusions reached above are not affected, as can be easily checked.

*c. Pyracene<sup>+</sup>*

With the aid of  $g_{\text{iso}} = 2.00268$  and the theoretical spin densities we calculated:

$$\begin{aligned} j_{\beta}^{\text{H}}(0) &= 588.8 + 132.3 (g_1 - g_2) \cdot 10^4 && \text{Hyperconjugation +} \\ j_{\delta}^{\text{C}}(0) &= 105.4 - 42.3 (g_1 - g_2) \cdot 10^4 && \text{induction} \end{aligned} \quad [11a]$$

$$\begin{aligned} j_{\beta}^{\text{H}}(0) &= 533.0 + 127.6 (g_1 - g_2) \cdot 10^4 && \text{Hyperconjugation} \\ j_{\delta}^{\text{C}}(0) &= 41.83 - 43.1 (g_1 - g_2) \cdot 10^4 && \end{aligned} \quad [11b]$$

$$\begin{aligned} j_{\beta}^{\text{H}}(0) &= 593.6 + 153.2 (g_1 - g_2) \cdot 10^4 && \text{Induction} \\ j_{\delta}^{\text{C}}(0) &= 210.0 - 47.3 (g_1 - g_2) \cdot 10^4 && \end{aligned} \quad [11c]$$

Since  $(g_1 - g_2) = 6 \times 10^{-4}$  (see ref. 23),  $j_{\beta}^{\text{H}}(0)$  is large and positive and  $j_{\delta}^{\text{C}}(0)$  small and negative.

The experimental spectrum observed in  $\text{H}_2\text{SO}_4$  (Fig. 3) shows that the principal  $^{13}\text{C}_{\delta}$  hyperfine line at high field has a higher peak height than the corresponding component at low field, hence this hyperfine component belongs to  $M(^{13}\text{C}) = +\frac{1}{2}$ . From this it follows that the sign of  $a_{\delta}^{\text{C}}$  is negative. The much higher peak height of the principal  $\beta$ -proton low-field hyperfine component compared with the corresponding high-field component is in agreement with the large positive value of  $j_{\beta}^{\text{H}}(0)$  and the negative sign of  $a_{\beta}^{\text{H}}$ .

(Received May 13th, 1971)

<sup>25</sup> J. R. Bolton and G. K. Fraenkel, *J.Chem.Phys.* **41**, 944 (1964).